Retention of Zinc and Chromium Ions by Different Phases of Hydrated Calcium Aluminate: A Solid-State ^{27}Al NMR Study

Isabelle Moulin,[†] William E. E. Stone,*[,†,‡] Jesus Sanz,[§] Jean-Yves Bottero,[†] Francis Mosnier,[⊥] and Claude Haehnel[||]

CEREGE, Equipe de Physico-Chimie des Interfaces, UMR 6635 CNRS/Université Aix-Marseille III, Europole de l'Arbois, BP 80, 13545 Aix-en-Provence Cedex 4, France, Section de Physico-Chimie Minérale, Musée Royal de l'Afrique Centrale, Campus de la Plaine, ULB, CP232, Brd du Triomphe, B-1050 Bruxelles, Belgium, Institut Cienca de Materiales, CSIC, Cantoblanco, 28049 Madrid, Spain, SITA, 94 Rue de Provence, 75009 Paris, France, and ATILH, La Défence 4, 7 Place de la Défence, 92974 Paris La Défence Cedex, France

Received: October 6, 1999; In Final Form: June 15, 2000

In cement-based materials, heavy metals are present in trace amounts. Depending on their mode of fixation and exact location in the solid, these metal ions may be released later into the environment. Solid phases formed during the hydration of tricalcium aluminate C_3A have been studied by ^{27}Al MAS NMR. It is shown that different layered AFm phases are formed depending on the nature of the charge-compensating anions incorporated into their interlamellar space. C_3A samples hydrated 15 and 72 h with and without metal ions have been examined and the results compared. Octahedral aluminum present in both the final hydrated form C_3AH_6 and AFm phases can be distinguished by the values of chemical shift and quadrupolar parameters (ν_q and η). Chromium ions substitute Al in both structures. Adsorption of CrO_4^{2-} and $Zn(OH)_4^{2-}$ ions at the interlamellar or external surfaces of the AFm phases seems to be favored. This leads during hydration to a temporary stabilization of the AFm phases relative to the final stable C_3AH_6 phase.

Introduction

Cement contains trace amounts of heavy metals of various origins. Heavy metals naturally present in some of the raw materials used for the manufacture of clinkers constitute the main source of contamination. The use of industrial waste as substitutes for fossil fuels is another important source.[1] During the hydration of cement, anhydrous phases dissolve and species in solution react to form hydrated products. So, whatever the location of the heavy metal in the anhydrous cement phase (within the crystal structure or present as metal oxide), it will certainly change during hydration. As cement is a complicated multiphase product, an interesting approach consists of studying the heavy metal retention in each of the hydrated cement phases. During the dissolution of tricalcium aluminate (which is the most important calcium aluminate phase of ordinary Portland cement), transient layered AFm phases are formed. These phases gradually disappear as hydration proceeds until the stable hydrated C_3AH_6 phase is formed. The structure of these AFm phases varies according to the nature (and degree of hydration) of the counterions, which compensate the positive charge of the layers of general composition $[Ca_2Al(OH)_6]^+$. Within the interlamellar space of an AFm phase, heavy metals may be retained. The presence of a small amount of metal ions may therefore considerably influence the hydration process of tricalcium aluminate. In this area NMR spectroscopy is extremely useful[2,3] as cement hydration leads to disordered phases that are often difficult to completely analyze by other methods such as X-ray diffraction. In a previous paper, lead and zinc retentions during hydration of tricalcium silicate were studied by ^{29}Si NMR spectroscopy.[4] The aim of this work is to study the retention sites of zinc and chromium in tricalcium aluminate hydrated phases. It will be shown that ^{27}Al MAS NMR provides structural information concerning the site localization of these trace elements and also a better understanding of how small amounts of metal ions may influence the hydration process of tricalcium aluminate.

Experimental Section

Materials. In this paper, three sets of samples have been studied. In the first two (set A and set B), samples were prepared starting from an initially nonhydrated tricalcium aluminate noted C_3A using the shorthand cement nomenclature (C, CaO; A, Al_2O_3; H, H_2O). The third (set C) consists of synthetic AFm phases. To prevent CO_2 contamination and precipitations of carbonates, all preparations were carried out in a glovebag under nitrogen as described below.

Set A noted $[C_3A + LW + Me]_{72h}$: C_3A is hydrated with lime water (LW) at a water/solid ratio equal to 10 to which either $Zn(NO_3)_2 \cdot 6H_2O$, $Cr(NO_3)_3 \cdot 9H_2O$, or $Na_2CrO_4 \cdot 4H_2O$ is added to obtain an initial metal concentration of 8×10^{-3} mol L^{-1}. A control sample (without any metal ion) was also prepared. The suspensions are then shaken (on a rotary shaker) for 72 h. After centrifugation (1 h, 50 000 rpm), the recovered solids are dried by acetone and the supernatants analyzed for Zn or Cr using an AA Hitachi spectrometer Z-8200.

Set B noted $[C_3A + LW + Me]_{15h}$: these samples were prepared as described above (set A) except that (i) the water/solid ratio was increased to 36, (ii) the initial metal concentration

* To whom correspondence should be addressed. E-mail: wstone@ulb.ac.be. FAX: 00/32/(0)2650 5023.
[†] CEREGE, Equipe de Physico-Chimie des Interfaces.
[‡] Musée Royal de l'Afrique Centrale.
[§] Institut Cienca de Materiales, CSIC.
[⊥] SITA.
[||] ATILH.

10.1021/jp993580z CCC: $19.00
Published on Web 09/13/2000

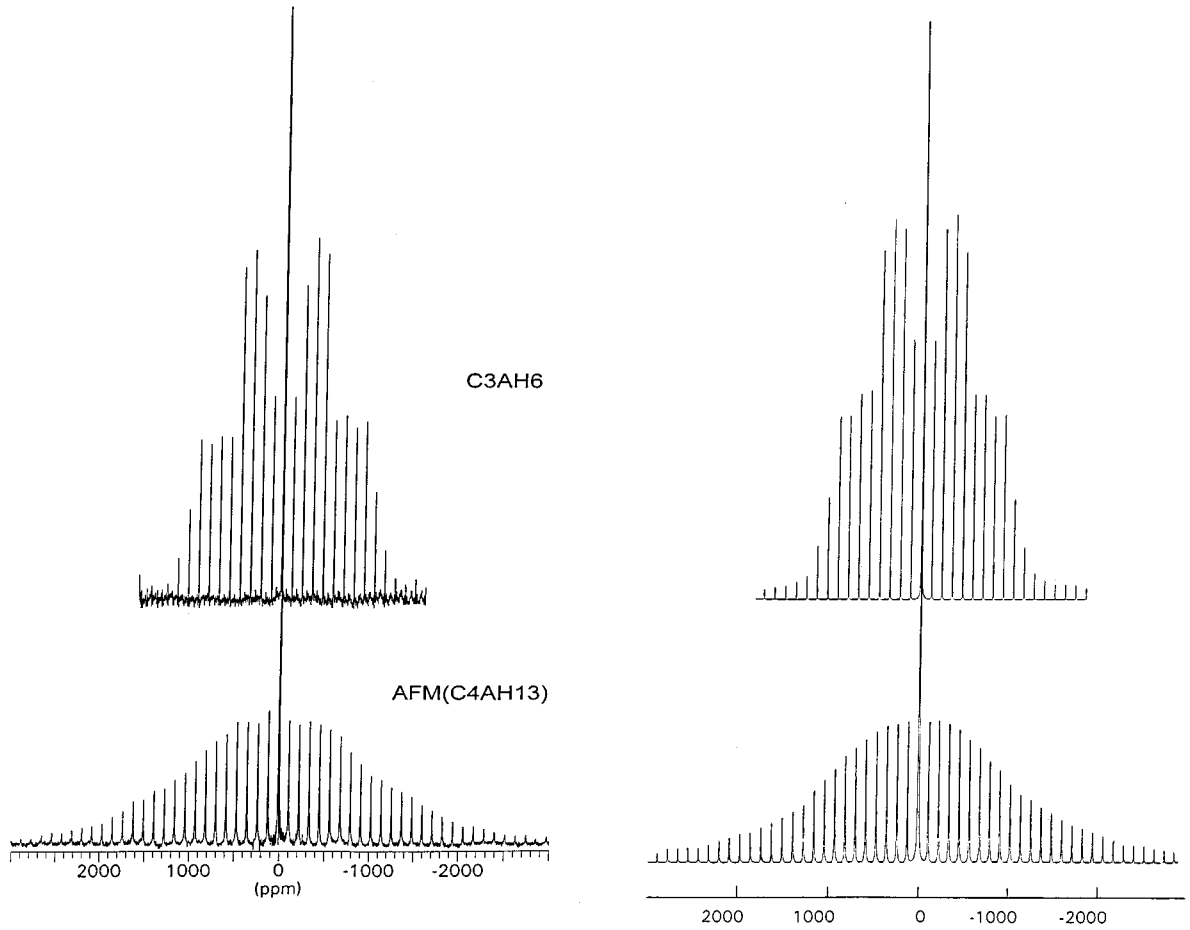

Figure 1. ^{27}Al MAS NMR spectra of (top) the final stable product C_3AH_6 and (bottom) a pure AFm phase C_4AH_{13}; left, experimental curves; right, simulated spectra.

was 5×10^{-3} mol L^{-1}, and (iii) the hydration time was reduced to 15 h. These modifications were made in order to increase both the metal content and amount of AFm-type phases.

Set C: four different AFm-type phase samples were synthesized and named AFm1 to AFm4 corresponding, respectively, to C_4AH_{13}, $C_3A{\cdot}CaCO_3{\cdot}11H_2O$, $C_3A{\cdot}CaCrO_4{\cdot}nH_2O$, and $C_3A{\cdot}Ca(NO_3)_2{\cdot}nH_2O$. AFm1/$C_4AH_{13}$: obtained by mixing in stoichiometric quantities $NaAlO_2$ and decarbonated CaO in an excess of ultrapure and decarbonated water. The suspension is stirred for 30 min and then let to stand for 12 h at 5 °C. The suspension is then filtered and dried by acetone and ether. AFm2/$C_3A{\cdot}CaCO_3{\cdot}11H_2O$: prepared by mixing in stoichiometric quantities $NaAlO_2$, $CaCO_3$, and decarbonated CaO in an excess of ultrapure and decarbonated water and stirring for 30 min. The suspension is filtred and the solid phase dried as above. The two other AFm-type phases, AFm3/$C_3A{\cdot}CaCrO_4{\cdot}nH_2O$ and AFm4/$C_3A{\cdot}Ca(NO_3)_2{\cdot}nH_2O$ were prepared in the same way as AFm2 by mixing in stoichiometric quantities, for the first $NaAlO_2$, $Na_2CrO_4{\cdot}4H_2O$ and decarbonated CaO, and for the second $NaAlO_2$, $Ca(NO_3)_2{\cdot}2H_2O$ and decarbonated CaO. Great care should be taken during the synthesis and conservation of these various phases especially for AFm1/C_4AH_{13}, which is very sensitive to carbonation and reverts quickly back to the cubic stable phase C_3AH_6. The purity of the AFm phases was controlled by X-ray diffraction (with a Philips PW 3710 X-ray diffractometer using a Co Kα radiation at 40 KV and 40 mA).

NMR Measurements. Solid-state ^{27}Al MAS NMR spectra were obtained with a Bruker MSL400 spectrometer. High-speed 5 mm spinning MAS rotors were used at 12 kHz. All spectra were obtained by a single excitation pulse with a pulse width of 1.5 μs (corresponding to a $\pi/10$ pulse), a 1.5 s recycle delay, and wide-band filtering (2 MHz). Baseline distortions were removed after correction for dead time effects. The 3QMAS spectrum was acquired on a Bruker AVANCE 400 WB spectrometer (at the Bruker plant Karlsruhe) with a 4 mm MAS rotor spinning at 14.5 kHz. Acquisition used a combination of Z-filtering, rotor synchronization, and hypercomplex phase cycling. The first and second pulse (widths, respectively, 2.6 and 0.9 μs) were applied with a radio-frequency field strength of 115 kHz while the third pulse was adjusted to selectively excite the central transition of the ^{27}Al spectrum. The recycle time was 1 s.^{27}Al chemical shifts are reported in ppm relative to an aqueous solution of $AlCl_3{\cdot}6H_2O$. The quadrupolar constants ν_q and η (where ν_q is the quadrupolar frequency defined as $3e^2qQ/h2I(2I-1)$ and η the asymmetry constant) are sensitive indicators of the distortion of the Al polyhedron and its immediate environment. When the quadrupolar interactions are relatively small (ν_q around 100−200 kHz), second-order quadrupolar effects are not too important and the MAS spectra are easy to recover. Spectral computer simulations were performed using the Bruker WIN NMR software package. Intensities, positions, and line widths (together with sample spinning rate) are determined with a nonstandard iterative least-squares method incorporated into the software package. The quadrupolar constants ν_q and η are, however, adaptable parameters determined by a trial-and-error procedure. Spectral fitting of the experimental NMR envelope is carried out by fitting each transition line separately (in this case, ($+^1/_2$, $-^1/_2$), ($\pm^1/_2$, $\pm^3/_2$), and ($\pm^3/_2$, $\pm^5/_2$)). An estimate of the second-order corrections to the value of the chemical shifts is obtained by

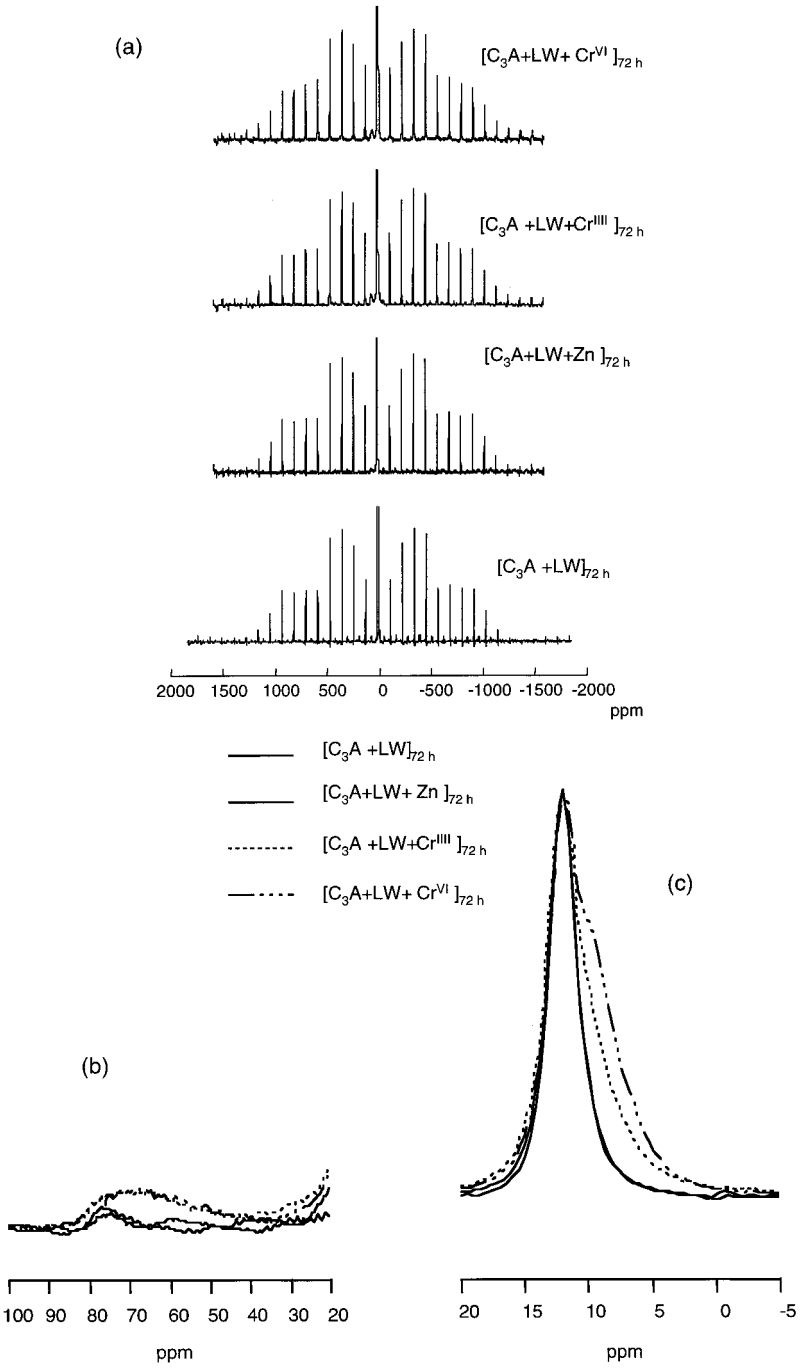

Figure 2. ^{27}Al MAS NMR spectra of samples of set A, i.e., $[C_3A + LW + Me]_{72h}$: (a) the spinning sideline spectra; (b) expansion of the central line region showing the tetrahedral lines; (c) expansion of the central line region showing the octahedral lines.

using the relation[5] $\delta_{iso} = \delta_{3/2} - (\delta_{3/2} - \delta_{1/2})/9$, where $\delta_{1/2}$ and $\delta_{3/2}$ are, respectively, the central positions of the $(+^1/_2, -^1/_2)$ and $(\pm^1/_2, \pm^3/_2)$ transitions. The relative intensities $I_{1/2}$:$I_{3/2}$:$I_{5/2}$ of the $(+^1/_2, -^1/_2)$, $(\pm^1/_2, \pm^3/_2)$, and $(\pm^3/_2, \pm^5/_2)$ lines (theoretically equal to 1:1.78:1.1) are also determined together with percentages of Al present in different phases. In general, spectral simulations are within less than 2% of the observed spectra. Estimated errors for the various extracted parameters are for the chemical shift, ±0.2 ppm; for η, ±0.1; and for ν_q, ±10 kHz.

Results

The initial nonhydrated C_3A was examined; its NMR spectrum is identical to the one already published by Skibsted[6] and shows the presence of two tetrahedral sites with isotropic chemical shifts at, respectively, 78.3 and 79.5 ppm. This spectrum can be used as reference to control if remains of nonhydrated C_3A are still present in the hydrated samples. As discussed above, hydration of C_3A leads to the successive formation of AFm and C_3AH_6 phases. In both cases Al is octahedral but characterized by a different chemical shift and quadrupolar constants. This is illustrated in Figure 1, which compares (together with their simulated spectra) the experimental spectra obtained for a pure AFm phase (C_4AH_{13}) with that of the final stable product C_3AH_6. For C_4AH_{13} (sample AFm1) the values obtained by spectral fitting are $\delta_{iso} = 10.8$ ppm, $\nu_q = 197$ kHz, $\eta = 0.5$, with relative intensities $I_{1/2}$:$I_{3/2}$:$I_{5/2} = 1$:1.6:0.4. For C_3AH_6 (the fully hydated C_3A sample) the values obtained are quite different: $\delta_{iso} = 12$ ppm, $\nu_q = 108$ kHz, $\eta = 0$, and $I_{1/2}$:$I_{3/2}$:$I_{5/2} = 1$:1.2:0.6. These differences will

TABLE 1: C_3A Samples Hydrated 72 h[a]

samples	δ_{iso} (ppm)	ν_q (kHz)	η	$I_{1/2}$:$I_{3/2}$:$I_{5/2}$	Al content (%) Al^{VI}[1]	Al^{VI}[2]	Al^{IV}	atomic ratio (%)
$[C_3A + LW]_{72h}$	12.5	108	0	1:1.2:0.6	100			
$[C_3A + LW + Zn]_{72h}$	12.5	108	0	1:1.2:0.6	100			Zn/Al: 1.1
$[C_3A + LW + Cr^{III}]_{72h}$	12.5	109	0	1:1.3:0.7	62			Cr/Al: 1.1
	10.5	180	0.5	1:1.0:0.3		31		
	±80	±760	0				±6	
$[C_3A + LW + Cr^{VI}]_{72h}$	12.4	108	0	1:1.5:0.7	46.3			Cr/Al: 1.0
	11	181	0.5	1:1.0:0.5		47		
	±80	±790	0				±7	

[a] Parameters obtained by simulation; for sample $[C_3A + LW + Cr^{III}]_{72h}$, the influence of a paramagnetic effect of Cr^{III} is ignored.

TABLE 2: C_3A Samples Hydrated 15 h[a]

samples	δ_{iso} (ppm)	ν_q (kHz)	η	$I_{1/2}$:$I_{3/2}$:$I_{5/2}$	Al content (%) Al^{VI}[1]	Al^{VI}[2]	Al^{IV}	atomic ratio (%)
$[C_3A + LW]_{15h}$	12.5	108	0	1:1.6:0.9	11			
	10.5	191	0.5	1:0.9:0.3		71		
	±80	±890	0				18	
$[C_3A + LW + Zn]_{15h}$	11	180	0.6	1:0.5:0.2		80.6		Zn/Al: 2.4
	±80	±840	0				19.4	
$[C_3A + LW + Cr^{III}]_{15h}$	10.8	180	0.5	1:0.5:0.4		81		Cr/Al: 2.3
	±80	±884	0				19	
$[C_3A + LW + Cr^{VI}]_{15h}$	10.9	185	0.5	1:0.5:0.2		80.2		Cr/Al: 2.2
	±80	±894	0				19.8	

[a] Parameters obtained by simulation; for sample $[C_3A + LW + Cr^{III}]_{15h}$, the influence of a paramagnetic effect of Cr^{III} is ignored).

show up in the results presented below; the results are discussed in a later section.

Set A: Samples Issued from the Hydration of C_3A during 72 h. The experimental spectra of the 72 h hydrated C_3A samples, $[C_3A + LW]_{72h}$ and $[C_3A + LW + Me]_{72h}$ (Me = Zn, Cr^{III} and Cr^{VI}), are given in Figure 2. The spectra shown in Figure 2a seem at first sight to be all quite similar. However a closer examination shows significant differences between samples $[C_3A + LW]_{72h}$, $[C_3A + LW + Zn]_{72h}$, and those containing chromium. For these latter samples, the outer spinning sidebands extend much further out in frequency, and the shape of their central lines located in the octahedral region (Figure 2c) is different. The presence in the spectrum of $\{C_3A + LW\}_{72h}$ of a very small set of spinning sidebands (corresponding to tetrahedral Al) is due to the presence of some impurity; its presence was disregarded as it has no influence on the general interpretation proposed in this paper. The central lines lines of both $[C_3A + LW]_{72h}$ and $[C_3A + LW + Zn]_{72h}$ are similar and symmetrical around 13 ppm; those of $[C_3A + LW + Cr^{III}]_{72h}$ and $[C_3A + LW + Cr^{VI}]_{72h}$ display a shoulder shifted toward 10 ppm. The spectra of these two latter samples show a small but clearly visible tetrahedral component (in the 50−80 ppm region, see Figure 2a,b). By simulation of the entire spectral region (using the procedure discussed above in the Experimental Section), the quadrupole frequency ν_q (kHz), asymmetry constant η, and relative intensities $I_{1/2}$:$I_{3/2}$:$I_{5/2}$ are determined. In the case of samples $[C_3A + LW + Cr^{III}]_{72h}$ and $[C_3A + LW + Cr^{VI}]_{72h}$, two octahedral sites plus a tetrahedral site Al^{IV} are introduced; for the two other samples, however, only one octahedral site is required. From the positions of the different transitions, a corrected isotropic chemical shift δ_{iso} (ppm) can be deduced. Values for these various parameters together with relative fractions of Al in different environments are given in Table 1.

Set B: Samples Issued from the Hydration of C_3A during 15 h. The spectra obtained for this series of samples are given in Figure 3. It is observed (Figure 3a) that compared to the previous series the intensities of the spinning sidelines manifolds are less important and follow a different pattern. Furthermore the spectrum of the control sample $[C_3A + LW]_{15h}$ is quite different from those of the other samples to which metal ions had been added. The central lines of all samples (Figure 3c) are very similar but now located compared to those of set A at a lower shift value (around 10 ppm). Except for $[C_3A + LW]_{15h}$, which contains two octahedral sites, all other samples could be fitted with just one octahedral site. Compared to set A, all samples have a much larger tetrahedral component (Figure 3b). The parameters extracted by simulation are given in Table 2.

TABLE 3: Synthetic AFm Phases (Parameters Obtained by Simulation)

samples	δ_{iso} (ppm)	ν_q (kHz)	η	$I_{1/2}$:$I_{3/2}$:$I_{5/2}$	Al^{VI}[2] content (%)
AFm1/C_4AH_{13}	10.8	197	0.5	1:1.6:0.4	100
AFm2/$C_3A{\cdot}CaCO_3{\cdot}11H_2O$	10.5	273	0.6	1:1.7:0.5	100
AFm3/$C_3A{\cdot}CaCrO_4{\cdot}nH_2O$	11.8	187	0.3	1:1.8:0.4	100
AFm4/$C_3A{\cdot}Ca(NO_3)_2{\cdot}nH_2O$	10.4	205	0.6	1:0.5:0.4	100

Set C: Synthetic AFm Phases. The ^{27}Al NMR results and parameters extracted by simulation are given, respectively, in Figure 4 and Table 3. It is observed that the spectra differ from sample to sample. The central lines located in the octahedral region (Figure 4b) have different values of chemical shift; ν_q is especially important for AFm2; relative intensities $I_{1/2}$:$I_{3/2}$:$I_{5/2}$ are similar for AFm1 to AFm3 but particularly low in the case of AFm4. All spectra could be fitted with a single octahedral component (see simulated spectrum of AFm1 in Figure 1).

Discussion

In lime water, the hydration reaction of C_3A can schematically be expressed as

$$C_3A \rightarrow C_4AH_{13}, C_4AH_{19}, C_2AH_8 \rightarrow C_3AH_6$$

The stable final C_3AH_6 phase has a cubic structure deduced from that of garnet ($Ca_3Al_2Si_3O_{12}$) with silicon ions left out and the charge balanced by hydroxyl groups (Figure 5b).[7] For

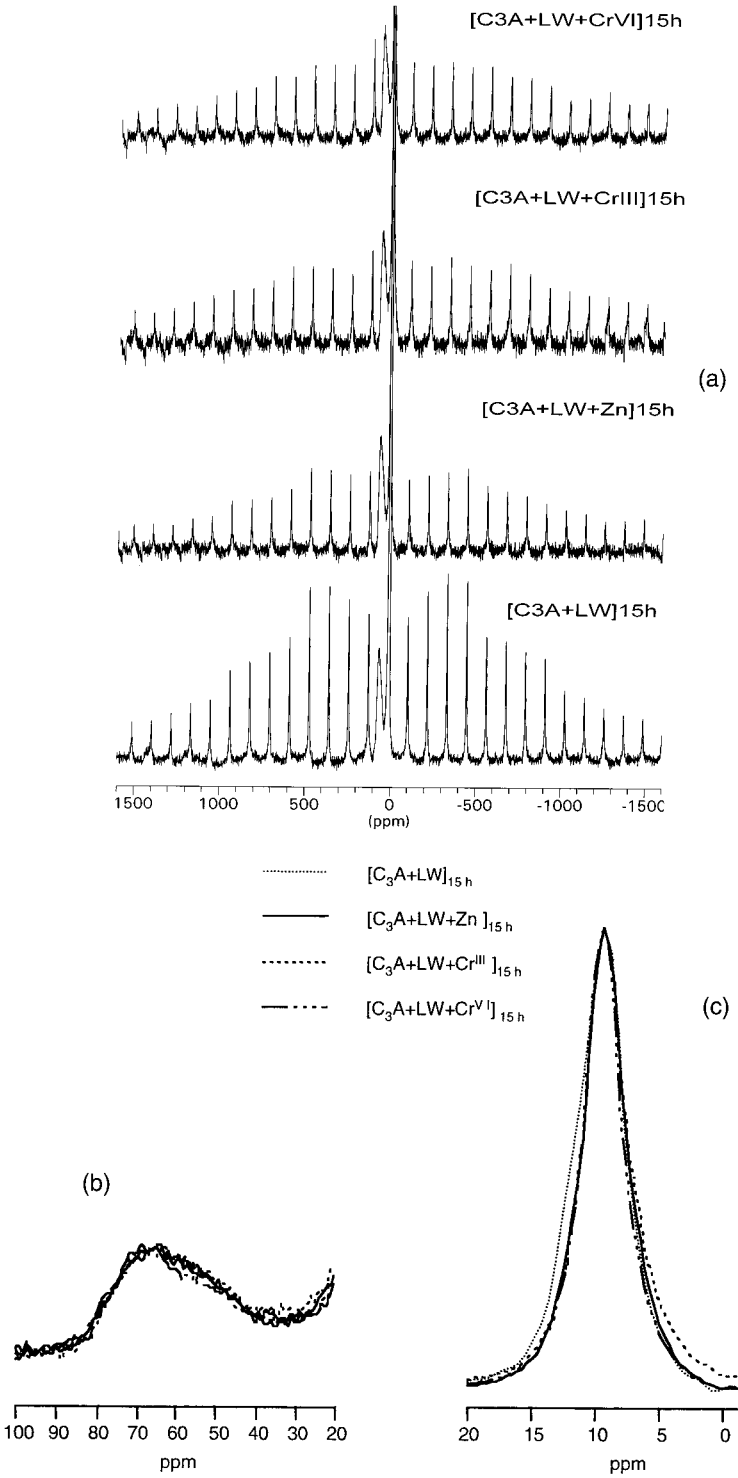

Figure 3. ^{27}Al MAS NMR spectra of samples of set B, i.e., $[C_3A + LW + Me]_{15h}$: (a) expansion of the spectra showing the inner spinning sidelines plus tetrahedral components; (b) expansion of the central line region showing the tetrahedral lines; (c) expansion of the central line region showing the octahedral lines.

the 72 h hydrated sample $(C_3A + LW)_{72h}$, the NMR parameters obtained by spectral simulation (see Table 1) are very close to those previously[3,8] obtained for C_3AH_6. Sample $(C_3A + LW)_{72h}$ has therefore been fully hydrated and its spectrum is composed solely (100%) of the symmetric ($\eta = 0$), not too distorted ($\nu_q = 108$ kHz), octahedrally coordinated Al with $\delta_{iso} = 12.5$ ppm (this site will be named Al^{VI}[1]). During hydration of C_3A, transient AFm-type phases of general formula $C_3A{\cdot}CaX_2{\cdot}yH_2O$[9] are formed. When hydration is conducted in lime water, X represents OH groups associated to Ca (for C_4AH_{13} and C_4AH_{19}).[10,11] However, depending on the hydration conditions (contact with atmospheric CO_2, presence of gypsum, of pollutants, ...), OH may be exchanged by different anions such as CO_3^{2-}, SO_4^{2-}, CrO_4^{2-}, and NO_3^-. The crystal structure of these lamellar calcium aluminate hydrates is based on the distorted brucite-like layers of composition $[Ca_2Al(OH)_6]^+$. The cavities between the main layers contain the charge-balancing X ions and some additional water molecules (Figure 5a).[12] These AFm phases are therefore expected to be present in the spectra of the less hydrated C_3A samples. Compared to what is observed

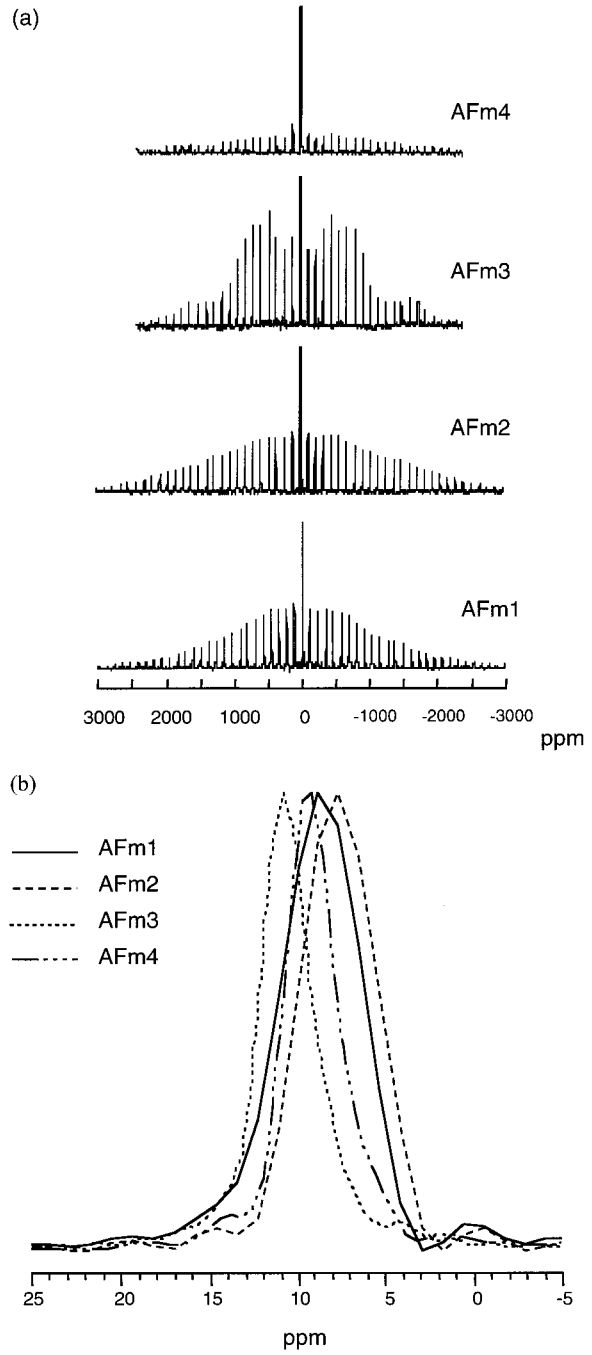

Figure 4. ^{27}Al MAS NMR spectra of the synthetic AFm-type phases (set C): (a) the spinning sideline spectra; (b) expansion of the central line region showing the octahedral lines.

for the 72 h hydrated samples, all 15 h samples have their central lines located at a much lower shift value (δ_{iso} around 11 ppm; see Figure 3). For the 15 h control sample $[C_3A + LW]_{15h}$, the spectral analysis, however, suggests the presence of two Al octahedral sites, one (11%) located at $\delta_{iso} = 12.5$ ppm corresponding to site $Al^{VI}[1]$ and a second (70−80%) more distorted site at $\delta_{iso} = 10.5$ ppm (named $Al^{VI}[2]$). The presence of this small amount of $Al^{VI}[1]$ can be detected in the spectrum by a slight shoulder of the central line around 13 ppm (see Figure 3c) but more characteristically by the two humps of the cubic C_3AH_6 phase clearly visible at ±500 ppm in the envelope of the spinning sidelines (see Figure 3a). As to the second Al^{VI}-[2] site, its NMR parameters are close (see above) to those found for the pure AFm phase C_4AH_{13} clearly indicating that after 15 h, the hydration process of C_3A has not reached its final state.

Identification of the AFm Phases Formed. To identify the AFm phase formed, four AFm samples with different anions were synthesized: C_4AH_{13}, $C_3A{\cdot}CaCO_3{\cdot}11H_2O$, $C_3A{\cdot}CaCrO_4{\cdot}nH_2O$ and $C_3A{\cdot}Ca(NO_3)_2{\cdot}nH_2O$ (AFm1 to AFm4). Their X-ray diagrams are given in Figure 6. Samples AFm2 and AFm3 show well-defined (001) peaks at, respectively, 7.6 and 10.2 Å indicative of the presence of only one AFm phase, i.e., $C_3A{\cdot}CaCO_3{\cdot}11H_2O$ and $C_3A{\cdot}CaCrO_4{\cdot}nH_2O$. They also contain trace amounts of Portlandite, calcite, and some residual chromium salt. As to AFm1 (C_4AH_{13}), the peak at 8.2 Å is skewed at about 7.9 Å with a small shoulder at 7.6 Å indicating that the AFm phase has been carbonated. The sample can therefore be considered as formed by a mixture of C_4AH_{13} (7.9 Å), $C_3A{\cdot}Ca.1/2CO_3{\cdot}11H_2O$ (8.2 Å) and $C_3A{\cdot}CaCO_3{\cdot}11H_2O$ (7.6 Å).[13] This carbonation probably occurred during the X-ray analysis which is not run under controlled atmosphere. For the NMR study, however, the sample was placed in the rotor directly after being dried with acetone, reducing in this case carbonation to a minimum. The X-ray diagram of AFm4 (having NO_3^{2-} ions in the interlayer space) shows the presence of two phases, one at 10.5 Å, the other at 8.5 Å. Following previous works,[14,15] the former should correspond to $C_3A{\cdot}Ca(NO_3)_2{\cdot}16H_2O$ and the second to $C_3A{\cdot}Ca(NO_3)_2{\cdot}10H_2O$. The peak at 7.6 Å due to carbonation is also present. The NMR spectra of all four samples were simulated (see Figure 1 for AFm1) using in each case a unique set of ν_q and η values. As shown by their spectra (Figure 4) and extracted parameters (Table 3), all samples show different NMR characteristics indicating that indeed both the nature of the interlayer ion and number of water molecules lead to structural modifications of the octahedrally coordinated Al polyhedra. It should be noted that except for sample AFm4 (which according to the X-ray results is certainly not pure) all other three AFm samples (see Table 3, fifth column) have relative intensities $I_{1/2}$:$I_{3/2}$ very close to the expected value (1.78). This shows that the structural heterogeneity of the Al sites is low and that only one AFm phase is present. Therefore AFm1 (C_4AH_{13}) has not been carbonated contrary to what happened during the time needed to record its diffraction pattern. In a previous NMR study of C_4AH_{13}, Skibsted et al.[8] could only simulate the observed spinning sidelines manifold of their sample by adding many spinning sideline spectra covering a range of different quadrupole parameters indicative of a highly disordered situation. The difference between our sample and the one analyzed by Skibsted is probably due to a difference in quality of the two samples. It is indeed very difficult to obtain a "pure" C_4AH_{13} phase free of any carbonation and without C_4AH_{19}. From Table 3, it can be seen that the quadrupolar values of $C_3A{\cdot}CaCO_3{\cdot}11H_2O$ are much larger than in the case of C_4AH_{13} and therefore a mixture of both phases would lead to a very heterogeneous situation. On the other hand by MQMAS NMR, Faucon et al.[3] interpreted the heterogeneity found in C_4AH_{13} as due to the presence of two polytypes. As stated above, for all $[C_3A+LW]_{15h}$ samples issued from the hydration of C_3A, the deduced NMR parameters for $Al^{VI}[2]$ are close to those of C_4AH_{13}. On the other hand, the corresponding relative intensities $I_{1/2}$:$I_{3/2}$:$I_{5/2}$ are significantly lower than those found for the synthetic AFm samples. Moreover the spinning sidelines corresponding to outer transitions display unusual shapes (the feet of the lines are asymmetrically broadened), which suggest the presence of different AFm phases having different crystallinity (during our simulations these lines were tentatively considered as being of Lorentzian shape). The presence of a heterogeneity of sites (i.e., structural disorder) with different quadrupolar constants leads to an appreciable increase in widths of the

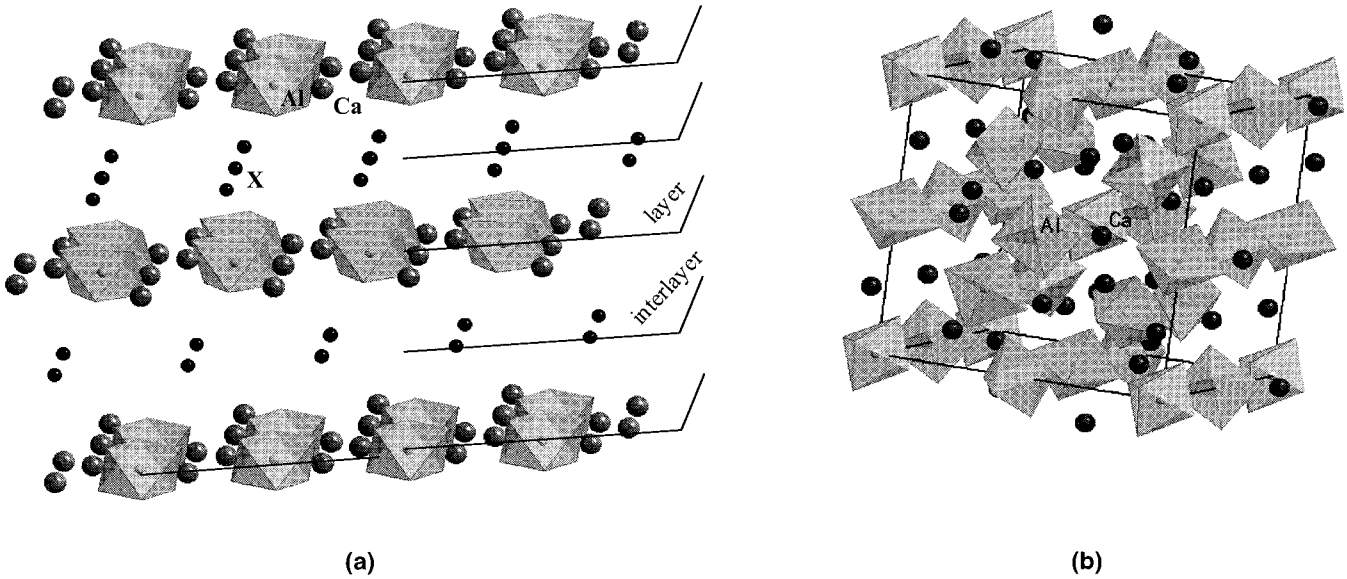

Figure 5. Schematic structures of AFm-type phases (a) and C_3AH_6 (b). Crystallographic data for C_3AH_6 taken from ref 7 and for the Afm phase from ref 12. Drawings made by Crystal Maker.

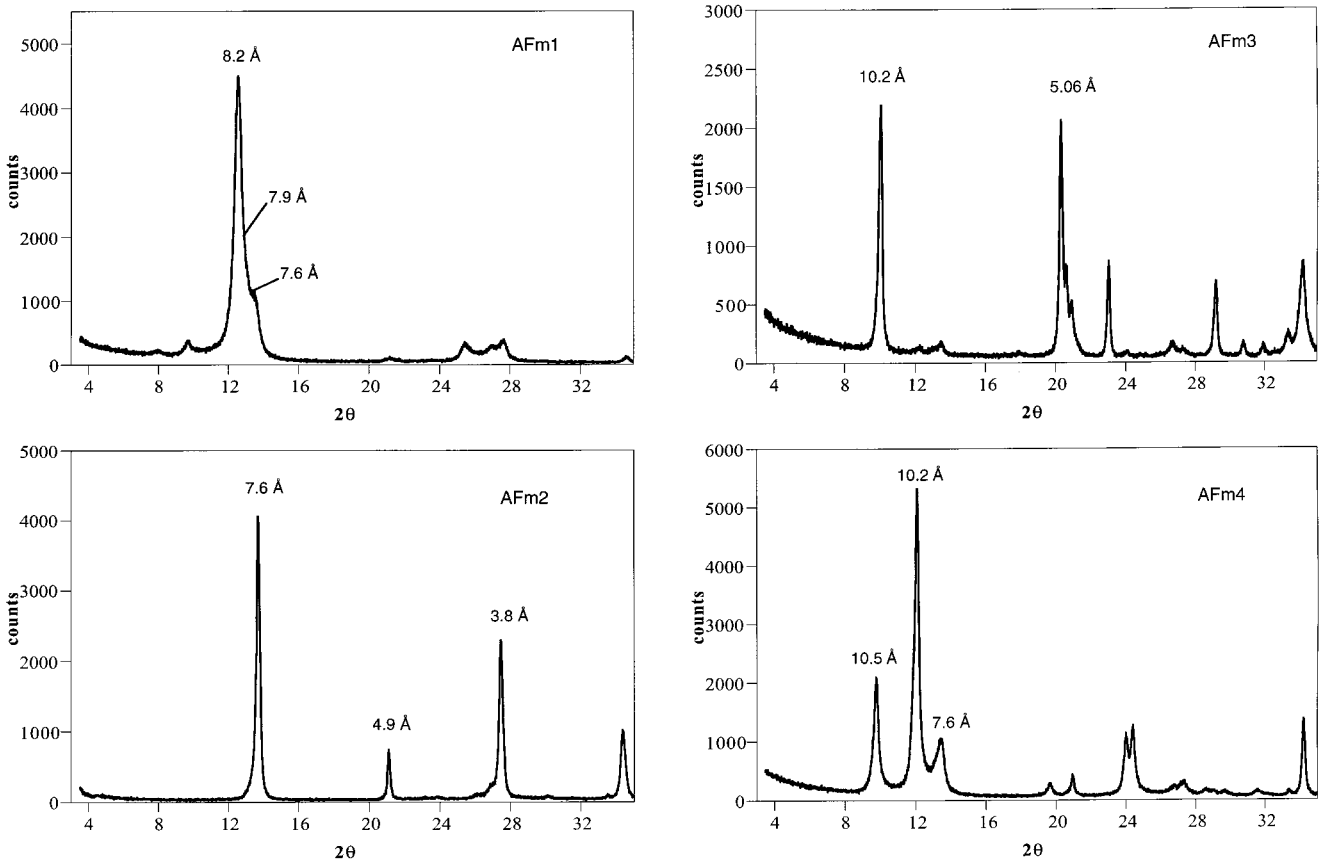

Figure 6. X-ray diagrams of the synthetic AFm-type phases (set C).

spinning sidelines making them much more difficult to detect. On the contrary, for a well-ordered crystalline phase such as powder corundum (having a much larger $\nu_q = 360$ kHz value), the values that we find for $I_{1/2}$:$I_{3/2}$:$I_{5/2}$ are very close to what is expected. Finally a small tetrahedral line Al^{IV} is present in the $(C_3A + LW)_{15h}$ spectrum but not in the synthetic AFm samples. According to a tentative second-order simulation of this tetrahedral component (during which η was arbitrarily set to zero), the value found for ν_q is large (890 kHz), which explains the difficulty in detecting the corresponding spinning sidelines. This tetrahedral line is also definitly different from that of the nonhydrated C_3A and therefore not indicative of the remains of the initial C_3A material. It should therefore be associated to tetrahedral Al present in the AFm phase (18% of the total detected Al).

The Effect of Zinc and Chromium Ions on the Hydration of C_3A. *(a) Zn.* The results for the 72 h hydrated C_3A with Zn are identical to those obtained by hydrating the sample without Zn (Table 1 and Figure 2). In both cases only the Al^{VI}[1] C_3AH_6 octahedral site is found present. This is probably due to

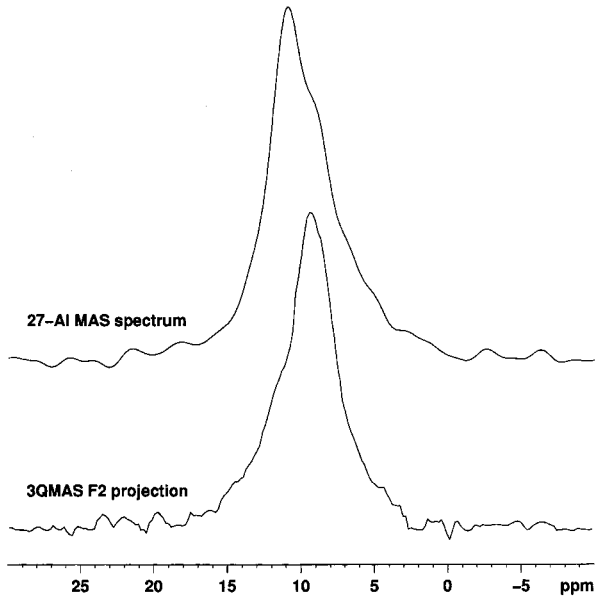

Figure 7. ^{27}Al NMR central line region of sample $[C_3A + LW + Cr^{VI}]_{72h}$ comparing (top), MAS spectrum; (bottom), 3QMAS F2 projection.

a precipitation of zinc as calcium hydroxizincate (or one of its precursors). For $[C_3A + LW + Zn]_{15h}$, however, the results are quite different (see Table 2 and Figure 3) from what is observed for $[C_3A + LW]_{15h}$. In presence of Zn and after 15 h, the C_3AH_6 phase is no longer detected; Al is now distributed between $Al^{VI}[2]$ (80.6%) and the tetrahedral line (19.4%) of the AFm phase that has been formed. The presence of $Zn(OH)_4^{2-}$ in the hydration medium of C_3A stabilizes the AFm phases at least for a short period as this effect is no longer visible after 72 h. Because precipitation of calcium hydroxyzincate is slow and not completed after 15 h, the amount of $Zn(OH)_4^{2-}$ ions remaining in the medium is sufficient to stabilize any existing AFm phase. *(b) Cr^{VI}.* Spectral simulation of the NMR envelope shows an equal amount of $Al^{VI}[1]$ and $Al^{VI}[2]$ for the 72 h hydrated sample $[C_3A + LW + Cr^{VI}]_{72h}$. Two features of the MAS spectrum indicate the presence of an $Al^{VI}[2]$ phase: (i) the central line displays a definite shoulder toward lower ppm values (see Figure 2c); (ii) the spinning sidelines extend over a much larger spectral range. The observed additional broadening of the central line could be interpreted as resulting from structural imperfections induced by Cr^{VI} ions. However a 3QMAS experiment carried out on this same sample clearly demonstrates the presence of a distinct separate AFm phase (with $\delta_{iso} = 10.5$ ppm as for all 15 h hydrated samples). Figure 7 compares the central region of the ordinary MAS spectrum with the result obtained along the anisotropic F2 dimension of the two-dimensional 3QMAS spectrum clearly showing the presence of a $Al^{VI}[2]$ line. $Al^{VI}[2]$ has a ν_q value practically double that of $Al^{VI}[1]$ (see Tables 1 and 2); its multiquantum detection selectivity is therefore much higher than that of the cubic $Al^{VI}[1]$ phase. Along the isotropic F1 dimension only a wide unresolved line is observed. The position of lines in F1 depends on the value of the chemical shift and ν_q of both sites. In this case a near superposition of lines giving a poorly resolved spectrum sum of the two contributions is observed. The relatively large intrinsic width of each line (due to a distribution of structural parameters for each site) adds to the loss in resolution found along F1. Along F2, however, the $Al^{VI}[2]$ line emerges because it is much more easily 3Q-excited than $Al^{VI}[1]$. A small amount (7% Al) of tetrahedral sites is also present in the MAS spectrum of this sample. Cr^{VI} (even at the very low concentration used here, 1 Cr^{VI} for 100 Al atoms) therefore stabilizes under hydration the AFm phases. The results for the 15 h sample $[C_3A + LW + Cr^{VI}]_{15h}$ are practically identical (Table 2) to those found for the other metal-containing samples, i.e., no $Al^{VI}[1]$ and approximately 80% of $Al^{VI}[2]$. For these samples the presence of AFm phases is preponderant. *(c) Cr^{III}.* Contrary to Cr^{VI}, Cr^{III} ions are paramagnetic, and the electron−nucleus interactions can lead to an additional broadening of the NMR lines as observed for sample $[C_3A + LW + Cr^{III}]_{72h}$ (see Figure 2c). This observation could be interpreted as resulting from a homogeneous distribution of Cr^{III} ions in the framework of the cubic phase. The substitution of octahedral aluminum by chromium in C_3AH_6 has indeed been suggested by others.[16] However, a small but nonnegligible amount of tetrahedral Al (6% Al) is also observed in the spectrum (Figure 2b) suggesting in line with our other results the presence of an AFm phase. Ignoring paramagnetic effects, the spectrum can then as previously be analyzed by spectral simulatation. The results given in Table 1 show that approximately one-third of the Al ions would then be located within the AFm phase. Because of possible paramagnetic effects, this amount of $Al^{VI}[2]$ is certainly smaller. For the 15 h hydrated sample $[C_3A + LW + Cr^{III}]_{15h}$ no broadening of the central line is observed (see Figure 3b) and the simulation now gives (see Table 2) 80% $Al^{VI}[2]$, the rest being located in tetrahedral sites. As for the other metal ions, the presence of Cr^{III} leads to a retardation in the hydration of C_3AH_6. The paramagnetic influence on the NMR signal of Al is greatly reduced if the Cr^{III} ions are closely packed. Cr^{III} is not very soluble at the pH value at which these samples are formed and could retain a hydroxide form which by adsorption stablizes the AFm phase.

Influence of the CrO_4^{2-} and $Zn(OH)_4^{2-}$ Anions on the Stuctural Stabilization of the AFm Phases. In hydrotalcites, CO_3^{2-}, SO_4^{2-}, and CrO_4^{2-} anions can be retained either within the interlayer space or on the external surface.[17] As hydrotalcite can be considered equivalent to an Al−Mg AFm phase, similar anionic retention sites are probably also present in our samples. Our results show (Table 1) that C_3A hydrated in the presence of CrO_4^{2-} for 72 h is formed by a mixture of C_3AH_6 and AFm components indicating that these latter lamellar phases are stabilized by the added CrO_4^{2-} ions. Dissolution of the AFm phases present in our samples probably occurs through the breakage of Al−O−Ca links located at the edges of the AFm layers. Adsorption of CrO_4^{2-} ions at these edge sites (i.e., on the external lateral surface) would then be responsible for the observed retardation in hydration. This external surface area only represents a small fraction of the total surface area of the sample (around 800 m^2/g as in the case of hydrotalcite). The average size of an AFm layer being approximately 1 μm,[9] the relative amount of aluminum atoms present at lateral faces (Al_L) with respect to the total number of aluminum (Al_T) is then of the order of 0.2%. Under our experimental conditions, the amount of CrO_4^{2-} present in the sample is sufficient to satisfy a one-to-one ratio between CrO_4^{2-} ion and Al_L. In this model, around 11% of the chromate ions are adsorbed on the lateral surface, the rest being essentially located in the interlamellar space. The anionic exchange capacity of the AFm phases calculated from the general formula $Ca_2Al(OH)_6 \cdot 2H_2O.^1/_2CrO_4 \cdot {}^7/_2H_2O$ is 260 mequiv/mol, which corresponds to 1 CrO_4^{2-} ion per 2 aluminum atoms. It should be noted that the molar ratio CrO_4 to Al of our samples is well below that of the anionic exchange capacity; i.e., the exchange capacity is far from being saturated. In the case of the sample $[C_3A + LW + Zn]_{15h}$, the AFm phases can also be assumed to be stabilized by adsorption

of $Zn(OH)_4^{2-}$ ions on sites present on the lateral faces. Nevertheless, in this case the interaction forces for these ions are less important than in the case of CrO_4^{2-} as no stabilization is found for samples hydrated 72 h.

Conclusions

Our results clearly show that during hydration metal ions even in very small amounts interact with the various existing phases present in the hydrated C_3A leading to observable site modifications of a major element such as aluminum. In the case of hydrated calcium aluminates, several metal retention sites have been identified. Chromium(III) could be homogeneously inserted into the structure of C_3AH_6, probably substituting in part for aluminum. Zinc and chromium ions stabilize the AFm phases by adsorption as $Zn(OH)_4^{2-}$ and CrO_4^{2-} ions on the lateral faces of the AFm layers. The CrO_4^{2-} ions also exchange hydroxyl groups present in the interlamellar space of the AFm phases. Many of the conclusions drawn here were only made possible by a detailed analysis of the entire ^{27}Al NMR spectrum.

Acknowledgment. The authors thank SITA, ATILH and ADEME for supporting this research. We would also like to thank Laurent Delevoye (Bruker France) for his help in retrieving the 3QMAS spectrum. During this work, W.E.E. Stone was invited as Professor at the University of Aix-Marseille and as Senior Researcher-CNRS.

References and Notes

(1) Moulin, I. *Speciation of Lead, Copper, Zinc and Chromium (III) and (VI) in Cement Hydrates*. Ph.D. Thesis, Université Aix-Marseille III, France, 1999 and references therein.

(2) Massiot, D.; Cote, B.; Taulelle, F.; Coutures, J. P. In *Application of NMR Spectroscopy to Cement Science*; Colombet, P., Grimmer, A. R., Eds.; Gordon and Breach Science Publishers: Langhorne, PA, 1994; p 153 and references therein.

(3) Faucon, P.; Charpentier, T.; Bertrandie, D.; Nonat, A.; Virlet, J.; Petit; J. C. *Inorg. Chem.* **1998**, *37*, 3726.

(4) Moulin, I.; Stone, W. E. E.; Sanz, J.; Bottero, J. Y.; Mosnier, F.; Haehnel, C. *Langmuir* **1999**, *15*, 2829.

(5) Jäger, C.; Kunath, G.; Losso, P.; Scheler, G. *Solid State Nucl. Magn. Reson.* **1993,** *2*, 73.

(6) Skibsted, J.; Bildsoe, H.; Jakobsen H. J. *J. Magn. Reson.* **1991**, *92*, 669.

(7) Weiss, R.; Grandjean, D.; Pavin, J. L. *Acta Crystallogr.* **1964**, *17*, 1329.

(8) Skibsted, J.; Henderson, E.; Jakobsen, H. J. *Inorg. Chem.* **1993**, *32*, 1013.

(9) Taylor, H. F. W. *Cement Chemistry*; Telford: New York, 1997.

(10) Scheller, T.; Kuzel, H. J. *Proceedings of the Sixth International Symposium on the Chemistry of Cement*; Academy of Science: Moscow, 1974.

(11) Richard, N.; Lequeux, N.; Boch, P. *Eur. J. Solid State Inorg. Chem.* **1995**, *32*, 649.

(12) Ahmed, S. J.; Glasser, L. S. D.; Taylor, H. F. W. *Proceedings of the Fifth International Symposium on the Chemistry of Cement*, Tokyo, 1968; Part 2, Supplementary Paper II-118.

(13) Fischer, R.; Kuzel, H. J. *Cem. Concr. Res.* **1982**, *12*, 522.

(14) Kuzel, H. J. *Proceedings of the Fifth International Symposium on the Chemistry of Cement*, Tokyo, 1968; Part 2, Supplementary Paper II-19.

(15) Dumm, J. Q.; Brown, P. W. *Adv. Cem. Res.* **1996**, *8*, 143.

(16) Kindness, A.; Macias, A.; Glasser, F. P. *Waste Manage.* **1994**, *14*, 3.

(17) Châtelet, L.; Bottero, J. Y.; Yvon, J.; Bouchelaghem, A. *Colloids Surf., A* **1996**, *111*, 167.